

Nanoscale fluoro-immuno assays with lanthanide oxide nanoparticles

I.M. Kennedy^{*a}, M. Koivunen^b, S. Gee^b, C. Cummins^a, R. Perron^a, D. Dosev^a, B.D. Hammock^b

^a Department of Mechanical and Aeronautical Engineering, ^b Department of Entomology
University of California Davis, Davis CA USA 95616

ABSTRACT

The use of polystyrene nanoparticles with europium chelate has been demonstrated as fluorescent reporters in an immunoassay for atrazine. The limit of detection with the nanoparticles was similar to that achieved with a conventional ELISA. It was shown that as the particle size decreased the time required for binding decreased and the sensitivity of the assay increased. This suggests that the use of smaller particles would greatly speed up the reaction and simultaneously increase sensitivity. However, the detection system used sets limits to the particle size as well. There is clearly a point where our detection system would not be sensitive enough to detect the emission from small particles. Therefore, a highly sensitive excitation/detection system needs to be developed to fully utilize the kinetic advantage from small particle size.

Keywords: immunoassay, nanoparticles, lanthanide, fluorescence, atrazine

1. INTRODUCTION

Immunoassays are biological assays, which use antibody/antigen recognition to detect and quantify target analytes. Immunoassays are used for both clinical and environmental monitoring. Enzyme-linked immunosorbent assay (ELISA) are competitive heterogeneous assays, which can be performed immobilizing one of the reagents on a variety of solid supports (tubes, microtiter plates, plastic-baked nitrocellulose membranes, magnetic particles, etc.). Measurements are based on light absorption proportional to color developed during the immuno reaction. Even though ELISAs are widely used, applications with fluorescent markers can increase sensitivity.

Microchannels, or lab-on-a-chip, have become a major thrust of biosensor research over the past decade owing to the use of smaller samples volumes and shorter assay times. Biological assays in microchannels have shown an increase in the assay sensitivity and a decrease in the assay time¹⁻⁸. The two major ways to construct microchannels are in a fully pre-sealed or detachable format. A pre-sealed channel is constructed using a photoepoxy such as Su8⁹ and all of the immunoassay steps are performed after the channel is constructed. An immunoassay using this type of channel has not been shown to be effective until recently¹⁰. The detachable channel uses poly(dimethylsiloxane) (PDMS) and is placed on top of a glass surface to create a sealable channel. This creates a channel where surface treatments to attach antibodies or antigens can be done prior to channel formation¹¹. More research needs to be done to optimize these biosensors for more specific applications. However, as science progresses future biological detection devices will use more microchannels to move the lab to a more mobile environment.

New labels can be useful in improving the sensitivity of fluoroimmunoassays. Polystyrene particles dyed with europium (III) chelates and europium (III) oxide nanoparticles have been shown to be effective fluorophores for time resolved fluorescence measurements in biological assays¹²⁻²¹. Europium(III) chelates – dyed polystyrene particles have major excitation peak at around 333 nm and fluorescence peak at 613 nm with a half life of 0.5 ms (Figure 1). Similarly, europium(III)oxide has excitation peaks at 280 nm, 394 nm and 466 nm with emission at 615 nm (Figure 2) and similar fluorescence lifetime. In contrast, most of the widely used organic fluophores have fluorescence lifetime in the pico- to nanosecond range. Thus, europium compounds are excellent markers for biological assays in which a clear differentiation between the signal and background is needed for increased sensitivity and detection. Recently,

* imkennedy@ucdavis.edu; Phone 530 752 2796; FAX 503 210 8220

nanoparticles containing europium have been shown to be effective fluorescent probes in immunoassays for prostate-specific antigen (PSA)^{13, 16, 17, 20} and a widely used herbicide, atrazine¹².

Herbicides and their metabolites in biological samples are good targets for immunoassays. Compounds such as atrazine or atrazine mercapturate can be detected using an ELISA or other immunochemical methods^{18, 22-24}. Atrazine (Figure 3) as a member of the triazine herbicide family is of interest because it is one of the most widely used herbicides in the US, and it has been shown to be present in groundwater²⁵. More importantly it has been shown to be a potential health risk to humans²⁶ as well as to interrupt the hormonal pathways in frogs²⁷. Current immunochemical methods have been able to detect atrazine at a concentration of $\sim 0.1 \text{ ng mL}^{-1}$ for a conventional ELISA²². In this work, a fluoro immuno assay for atrazine was developed using polystyrene – Eu(III) chelate particles for fluorescent reporters. The assay was optimized 96 –well plate and on waveguide as a first necessary steps for assay in a microchannel. The present study seeks to combine the advantages of lanthanide nanoparticle labeling in a fluoroimmunoassay with a microchannel-based assay. The efficacy of the approach is demonstrated first with an assay for atrazine on an indium tin oxide (ITO) surface where issues of non-specific binding can be addressed.

2 MICROCHANNEL DESIGN

A microchannel (0.8mm x 50mm x 16mm) has been proposed for heterogeneous immunoassays with configuration shown in Figure 4. The proposed microchannel consists of an indented layer of PDMS that creates a channel when covered over an indium tin oxide (ITO) coated glass. ITO has been shown to be an effective medium for the assembly of self-assembled monolayers (SAMs)²⁸⁻³⁰ due to the high surface density of hydroxyl groups. Preliminary studies revealed that ITO was the only substrate to effectively avoid sticking of the polystyrene particles. The PDMS system is advantageous because the ITO cleaning and hapten attachment can be performed prior to forming the channel. The proposed channel is designed for excitation with laser beam where the europium particles would be excited by light in the ultraviolet (UV) range through the PDMS (optically transparent down to 230nm); the europium particles will emit visible light which will be transmitted by the glass.

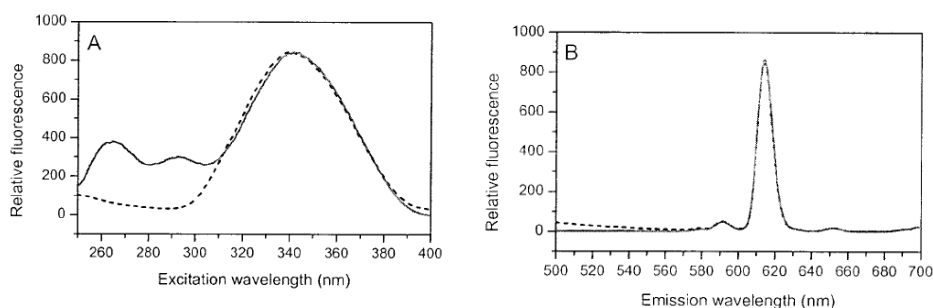


Figure 1. Fluorescent excitation (A) and emission (B) of polystyrene nanoparticles dyed with europium chelate (solid line) and europium chelate ions (dashed line)¹³.

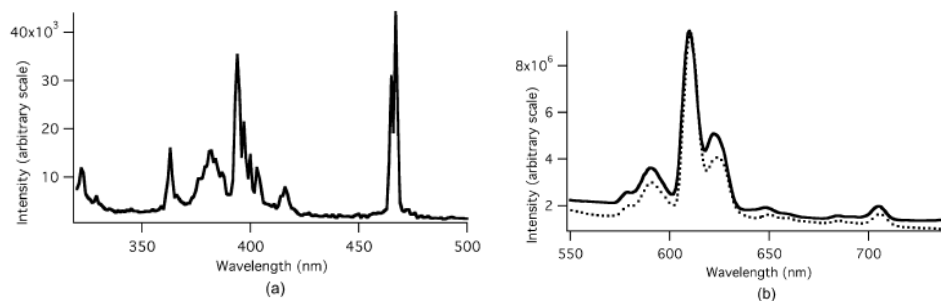


Figure 2. Excitation spectrum of Eu₂O₃ observed at 610 nm (a); emission spectrum of Eu₂O₃ (b) with excitation at 466 nm (solid curve – functionalized particles, dashed curve – bare particles)¹².

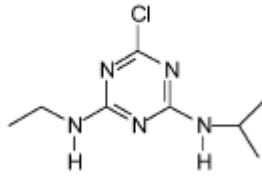


Figure 3. Structure of atrazine.

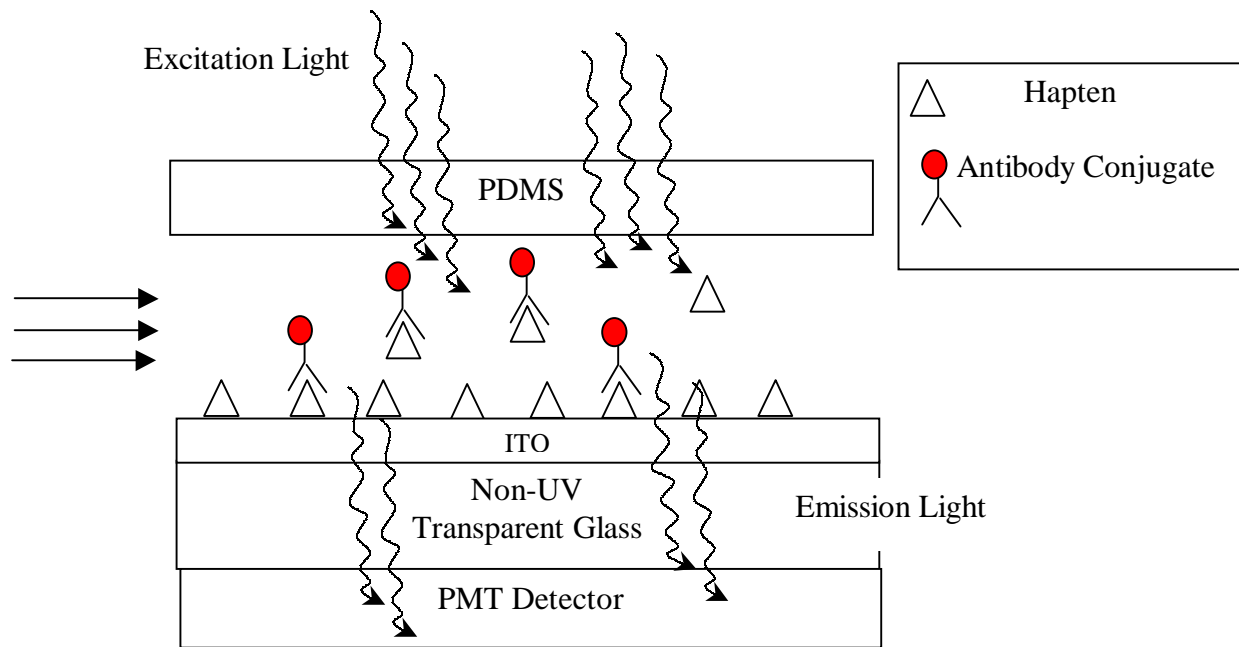


Figure 4. Proposed Microchannel for a Laser/PMT Set-up

3 ATRAZINE IMMUNOASSAY ON AN ITO-COATED WAVEGUIDE

As a first necessary step for the development of immunoassay in a microchannel, we have developed a competitive immunoassay for atrazine using an ITO coated waveguide as a solid support. For maximum sensitivity, polystyrene nanoparticles with europium chelate (Seradyn, IN) attached to monoclonal anti-atrazine antibodies were used as fluorescent reporters. Based on the initial tests determining the binding kinetics of antibody-nanoparticle conjugates, the 107-nm Seradyn particle was chosen as the ideal candidate to be incorporated into the competitive immunoassay. We have also evaluated regeneration methods in order to make the immunosensors more cost effective.

3.1 Materials and Methods

3.1.1 Antibody Coupling to Nanoparticles

Europium(III) chelate polystyrene nanoparticles (1% solids; 107-nm, 304-nm, and 396-nm) were supplied by Seradyn Inc., Indiana. The particles were attached to goat anti-rabbit IgG (Sigma, St. Louis, MO) or to Protein-A purified monoclonal anti-Atrazine antibody (AM7B.2) raised previously by Karu et al.²³ using a modification of a previously described method¹³. The particles were pre-washed on a Nanosep centrifugal filter membrane with 500 μ L 50 mM

phosphate buffer, pH 7.0. A particle concentration of $3\mu\text{g mL}^{-1}$ in 50 mM phosphate buffer was added to a 200 μL solution of 5 mg *N*-(3-dimethylaminopropyl)-*N*-ethylcarbodiimide (EDAC) and 5mg *N*-hydroxysulfosuccinimide (Sulfo-NHS) (Sigma, St. Louis, MO) per mL and rotated for 30 minutes to activate the carboxyl groups on the nanoparticle. The activated particles were washed twice with 50mM bicarbonate buffer, pH 8.5. A concentration of 1.13ng mL^{-1} AM7B.2 or $330\mu\text{g mL}^{-1}$ of goat anti-rabbit IgG antibody were incubated with the nanoparticles for 2 hours in 100mM bicarbonate buffer, pH 8.3. They were washed two times with 50mM bicarbonate buffer, pH 8.5 suspended in 300 μL of bicarbonate buffer, and stored at 4°C.

3.1.2 Competitive assay kinetics in a 96-well plate

In order to determine the optimal particle size for the waveguide assay, the effect of particle size on binding was analyzed using a 96-well plate. Nunc Maxisorp 96-well plates (Nunc, Roskilde, Denmark) were coated overnight at 4°C with 0.1mL per well of $3.25\mu\text{g mL}^{-1}$ of rabbit IgG (Sigma, St. Louis, MO) in carbonate-bicarbonate buffer (15mM Na_2CO_3 , 35mM NaHCO_3 , pH 9.6). The plates were washed three times with PBST (PBS plus 0.05% Tween 20) and blocked for one hour at room temperature with 0.5% ovalbumin in PBS. Anti-IgG coupled nanoparticles (4.125 μg of particles per well: 107-nm, 304-nm, 396-nm) were incubated in triplicate for 30 seconds to 2 hours and washed three times with PBST. The fluorescence intensities were read on a Spectrafluor Plus plate reader (TECAN Systems Inc., CA) with excitation/emission of 330/620nm. A standard competitive inhibition assay was performed to analyze the particle size effects on the signal to noise ratio (SNR) and on the IC_{50} , the point of 50% inhibition. Plates coated and blocked with the previously described method were incubated for one hour with equal volumes of $41.25\mu\text{g mL}^{-1}$ of coupled anti-IgG (107-nm, 304-nm, 396-nm) plus IgG (serial dilution: $130\mu\text{g mL}^{-1}$ of IgG diluted 1:10 to $1.3 \times 10^{-7}\mu\text{g mL}^{-1}$). The plate was washed three times with PBST and read using the plate reader and excitation/emission conditions indicated above.

3.1.3 Theoretical Flux Calculation

In order to determine the effect of particle size on binding kinetics, Ficks's law (Equation 1) was used to estimate the nanoparticles flux to the ITO surface.

$$J = \frac{\sqrt{D}}{\sqrt{\pi t}} C \quad (1)$$

For equation 1, C is the particle concentration, t is the time, and the D is the diffusivity. The diffusivity for a spherical particle was determined for each particle (2r = 107 nm, 304 nm, 396 nm) using equation 2

$$D = \frac{k_B T}{6\pi\eta r} \quad (2)$$

where k_B is the Boltzman constant, η is the viscosity of water at temperature (T) of 25°C. Water was chosen as a theoretical medium because the concentration of solutes in solution is minimal and hence, does not alter the physical properties of the medium significantly.

3.1.4 Antibody Surface Density Quantification

A combination of 30 μL of IgG-polystyrene fluorescent particles (Seradyn Inc.) conjugates (107 nm, 304 nm, and 396 nm were incubated separately), 300 μL of 50mM sodium bicarbonate (pH 8.5), and 25 μL of $560\mu\text{g mL}^{-1}$ rabbit IgG coupled to an Alexa Fluor 488 (Molecular Probes, OR) were mixed in a rotary mixer for one hour. The samples were centrifuged at 16.1×10^3 g for three minutes after which the supernatant was removed and the particles were washed with 500 μL of 50mM sodium bicarbonate, pH 8.5. The washing process was repeated and the pellet was re-suspended in 100 μL of 50mM sodium bicarbonate. The fluorescent emission of this suspension was read using an excitation/emission of 485/519nm on a SPECTRAMax M2 plate reader (Molecular Devices, Menlo Park, CA). The antibody surface density was determined against a standard curve with known concentrations of Alexa-IgG conjugate and the density was expressed as ng of protein per surface area.

3.1.5 ITO Regeneration

The waveguides were cleaned using an RCA method ($\text{H}_2\text{O} : 30\% \text{H}_2\text{O}_2 : \text{NH}_3$; 5:1:1 v/v/v; sonicated at 60°C for 30 min). They were then rinsed with excess deionized water and dried under vacuum at 120°C . During the testing, the waveguides were washed three times with PBST in-between each step. A concentration of 0.2mg mL^{-1} of IgG in 2-(4-Morpholino) ethanesulfonic acid (MES), pH 6.0, was incubated for ten minutes on the ITO waveguides. The waveguides were then washed three times with PBST after which they were blocked for ten minutes in a solution of 1% BSA in 50mM sodium bicarbonate, pH 8.5. After washing three times with PBST, 0.22mg mL^{-1} Alexa Fluor 598 goat anti-rabbit IgG (Molecular Probes, OR) in 50mM sodium bicarbonate plus 0.05% Tween 20, pH 8.5 was added on the surface, and incubated for 10 minutes. A fluorescence reading was taken at 330nm/620nm excitation/emission on a SPECTRAmax M2 plate reader (Molecular Devices, Menlo Park, CA). The waveguides were then washed three times in one of the following solutions: 0.1M Glycine-HCl, 0.05M NaOH, 0.16M NaOH, 0.45M NaOH, 10% Ethylene Glycol, 70% Ethanol, 1x PBS, 5x PBS, 10x PBS, and PBST. After washing, the waveguides were re-incubated with $20\mu\text{L}$ of 0.22mg mL^{-1} Alexa for 10 minutes and another fluorescence reading was taken. This cycle was repeated until there was basically no recognition of the anti-IgG to the IgG on the waveguide surface.

3.2.1 Competitive Atrazine ELISA on a 96-well plate

A solid phase indirect competitive ELISA was used for measurement of atrazine. Nunc MaxiSorb 96-well plates (Nunc, Roskilde, Denmark) were coated overnight at 4°C with the coating antigen Az-C4-Ova (1/18,000 dilution) in a 0.05 M sodium carbonate-bicarbonate buffer (pH 9.6). The following day, the coating antigen was washed off the plate with a phosphate buffer saline solution (PBS, pH 7.5) containing 0.05 % Tween 20, and the plate was blocked for one hr with 0.5 % Ovalbumin in PBS. After washing, $50\mu\text{L}$ of each standard in triplicate was pipetted into each well. The standard curve for atrazine was prepared from the stock standard ($1\mu\text{g mL}^{-1}$ atrazine in MeOH) and contained 0 – 250 ng of atrazine in one mL PBS containing 0.05 % Tween 20. To each sample well $50\mu\text{L}$ of the anti-atrazine monoclonal antibody (AM7B.2) was added in 1/1000 dilution, and the mixture was incubated at room temperature for one hour. The sample matrix was washed away leaving only the antibodies bound to the coating antigen. Then, $100\mu\text{L}$ of the anti-mouse IgG-horseradish peroxidase conjugate (1:5500 dilution; Sigma, St. Louis, MO) was added into each well, and the IgG-HRP was allowed to bind to IgG sites on the bound antibodies for 60 min. Unbound IgG-HRP was washed away to leave an amount of HRP enzyme that was inversely proportional to the atrazine concentration in the samples or standards. Finally, a colorless substrate, 1 % H_2O_2 , and a chromogen, tetramethylbenzidine (TMB) were incubated with the bound enzyme to produce a blue color. A $50\mu\text{L}$ aliquot of 2 M H_2SO_4 was added as a stop solution to change the color to a stable yellow. ELISA absorbances at 450 nm were measured with a SpectraMax2 microplate reader (Molecular Devices, Menlo Park, CA). The software package Softmax (Molecular Devices) was used for fitting the 11-point sigmoidal standard curve based on a four-parameter logistic method of Rodbard³¹.

3.2.2 Competitive Atrazine Immunoassay on an ITO Waveguide

ITO waveguides (ITO coated quartz, Delta Technologies Limited, MN, 1cm x 1cm) were cleaned using the previously described RCA method after which they were incubated with $30\mu\text{L}$ of $24\mu\text{g mL}^{-1}$ of atrazine coating antigen (Ova-C4-Atrazine) for 15 minutes and then blocked for 30 minutes with 1% BSA in 50mM sodium bicarbonate, pH 8.5. A 1:1 ratio of $0.55\mu\text{g mL}^{-1}$ of Seradyn 107-nm-IgG conjugates and 0, 0.1, 1, 10, 100, 10000 ng mL^{-1} of atrazine were pre-incubated overnight at 4°C . An aliquot of $30\mu\text{L}$ of the preincubated mixture was then placed on the waveguides for 30 minutes. A fluorescence reading was taken at 330nm/620nm excitation/emission on a SPECTRAmax M2 plate reader (Molecular Devices, Menlo Park, CA). The waveguides were washed three times with PBST in-between each incubation step.

4 RESULTS AND DISCUSSION

4.1 Binding kinetics in a 96-well plate

Experimental. An IgG/anti-IgG kinetic assay showed that as the particle size decreases the binding of the particle conjugate to the IgG surface increases (Figure 5). These intensities were converted into number of particles (Figure 6) by using a standard curve to relate intensity to particle mass and then further to number of particles based on relationship determined by Harma et. al¹³. This conversion was necessary because the number of particles varied between sizes although masses were constant. The slopes of the linear regions (3.13, 0.44, 0.11 particles bound min^{-1} for 107-nm, 304-nm, and 396-nm, respectively) of the three binding curves in Figure 7 increase with decreasing particle size, which

shows that smaller particles reach equilibrium more quickly. This phenomenon could be caused by faster binding because the smaller particles have a higher diffusivity. It could also be a direct result of better recognition due to the antibody surface density on the particle or interference of the particle label with the antibody binding reaction.

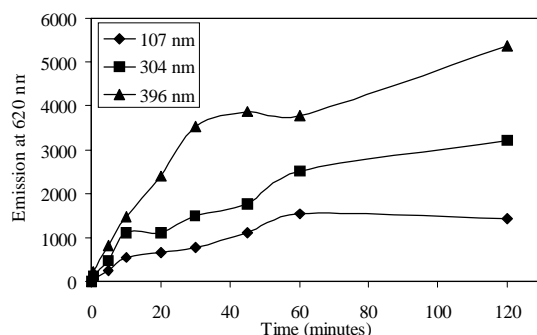


Figure 5. The fluorescence intensities of 107-nm, 304-nm, and 396-nm particles coupled to goat anti-rabbit IgG as a function of time. The assay was performed in a 96-well plate coated with IgG.

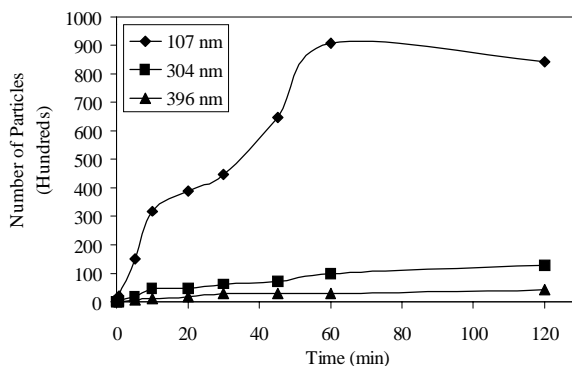


Figure 6. The effect of particle size on the number of particles bound on the surface of a 96-well plate coated with IgG

Theoretical. Our experimental findings support previously reported results with nano-particulate conjugates exhibiting significantly slower reaction rates than standard fluorophores³². According to Fick's Law (Equations 1 and 2), the increase in particle size results in a decrease in particle flux to the surface. As the particle size increases the particle flux decreases, confirming that the size of the particle affects the kinetics as expected. This supports previous findings on the kinetics of particles^{32,33} and the experimental observations in this study. However, the issue of antibody surface density needs to be examined to determine whether the faster binding of small particle conjugates is due to higher density of antibodies on the particle surface or to the fact that smaller particles have higher diffusivity with less steric hindrance.

Antibody surface density. In order to better understand the differences in binding kinetics, the antibody surface density for each particle size was determined (Table 1). The 107-nm particles had the lowest antibody density on the surface whereas the values for the two larger particles were higher with no significant differences between sizes. Even though differences in antibody surface densities were expected, we did not expect any trend among different particle sizes. The result shows that the fast rate of binding of the 107-nm particle conjugate is not due to the antibody surface density, but is a result of the smaller particle size. It has been reported using a sandwich assay that increasing the number of active sites (a value which is proportional to surface density) on a 107-nm Seradyn particle increases the association rate thirteen times¹⁷ and the detection limit five times¹⁹. Another report using 220-nm diameter fluorescent diameter microspheres shows that increasing the number antibodies on the particle surface increases the assay sensitivity³³. Our findings show that a higher surface density on a larger particle, i.e., density of active binding sites, does not outcompete

the effect of particle size on the binding rate. The rate of antibody/antigen binding seems to be primarily regulated by the particle size and hence, smaller particles are more suitable for competitive assays.

Table 1. Surface density of goat anti-rabbit IgG coupled to 107-nm, 304-nm, and 396-nm Seradyn particles.

Particle Size (nm)	Surface Density (ng nm ⁻²)
107	6.52 x 10 ⁻¹⁵
304	1.39 x 10 ⁻¹⁴
396	1.35 x 10 ⁻¹⁴

Competitive inhibition assay on a 96-wellplate. A high signal-to-noise ratio (SNR) accompanied by a low IC₅₀ value and low background is a requirement for a sensitive competitive ELISA. According to our results from a standard anti-IgG/IgG inhibition assay, particle size affects the SNR (Figure 7). The 107-nm particle conjugates had the highest SNR ratio, 10.5, while the 304-nm and 396-nm particles had an SNR of 2.2 and 2.0, respectively. Similarly, it can be concluded from Figure 7 that the background noise increases with particle size. For all the particle conjugates tested the IC₅₀ increased with decreasing particle size (IC₅₀: 571, 210, 0.7 ng/mL for 107, 304, and 396-nm, respectively). It is of interest to note that the 304-nm and 396-nm particles had a very high degree of variability within experiments, which is demonstrated by the poor fit of the 4-parameter curves: R²: 0.839 and 0.890 for 304-nm and 396-nm particles, respectively. Based on these results, the 107-nm particle would be best suited for a competitive immunoassay on a waveguide; it is the fastest, quite sensitive, and least variable. To support this conclusion, Koskinen et al.³² have reported that particle labels decreased the limit of detection (LOD) by two orders of magnitude using a 75-nm diameter particle in a sandwich assay in an ArcDia TPX bioaffinity system. Similarly, another study has shown using larger nanoparticles (220-nm) in a heterogeneous sandwich assay for IgG/anti-IgG that the LOD was 250 fold lower when compared to an organic dye reporter³³. Therefore nanoparticles are excellent candidates for labels in biosensors because they can help to increase the sensitivity. Based on the experimental results it is theorized that as the particle size decreases the SNR would increase. However, since the fluorescence intensity decreases with decreasing particle size, there is a point where a more sensitive fluorescence detector would be needed to detect a signal. This phenomenon needs to be further studied to determine the optimal particle size for the IgG model and subsequently for other molecules of interest.

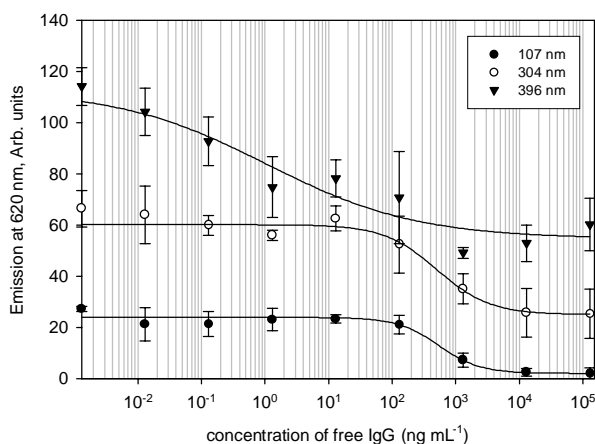


Figure 7. A 4-parameter curve fitting for the competitive inhibition of goat anti-rabbit IgG coupled to 107 nm, 304 nm, and 396 nm particles with free IgG (A: The highest emission; B: Slope of the linear region; C: IC₅₀ value; D: The lowest emission)

ITO Regeneration. With a successful regeneration, only the bonds between antigen and antibody are disrupted leaving the coating antigen intact on the ITO surface. Tests were conducted with several solvents to attempt to regenerate the ITO surface without stripping off IgG. It was shown that 0.1M Glycine-HCl and 0.16M NaOH were the most effective regeneration agents (Figure 8). However, it can be seen that the variability is extremely high for the 0.1M Glycine-HCl. ITO surfaces degrade under certain acid treatments³⁴⁻³⁶ and this could explain the large degree of variability within this treatment. The other solvents tested including a range of different concentrations of NaOH were not effective (data not shown). Using NaOH provided a surface that had 50% of the active surface remaining. The biosensor could still be used; however, the sensitivity and LOD will decrease with each regeneration cycle. After three regeneration cycles the surface seems to become inactive and the ITO needs to be reactivated using an RCA treatment.

Competitive assay using a waveguide. Preliminary tests for an IgG/anti-IgG and an atrazine immunoassay that incorporated different immobilization methods such as silane layers, dextran, and glass were shown to be incapable of reducing the non-specific binding of particles whereas ITO eliminated the non-specific binding. Our tests on a 96-well plate revealed that a competitive atrazine assay using particle labels was not successful for the same reason. Taking this into account, the ITO waveguides were selected as a surface for the immunoassay with 107-nm particle conjugate. A competitive immunoassay for atrazine was successfully performed using ITO coated glass as a solid support (Figure 9). The IC50 (~1 ng mL⁻¹) was calculated based on 50 % fluorescence inhibition. This is higher than in a standard 96-well competitive assay (0.143ng mL⁻¹) as shown in Figure 10, but it still has a reasonable detection level and shows the potential for ITO as a candidate for a biosensor. Other studies have shown a LOD of ~0.1ng mL⁻¹ for a conventional ELISA²² and ~0.5ng mL⁻¹ for a competitive immunoassay with magnetic separation¹². There are many factors that influence the difference between these two values. As shown before, the slower particle binding rate compared to an enzyme could affect the binding properties during the competition³². Future tests should examine if longer incubation times would decrease the IC50 and make the assays more sensitive. However, the purpose of this research was to develop a quick immunoassay to be used within a biosensor system. Therefore, optimizing the surface density would probably be a more effective way to increase the sensitivity and to decrease the assay time as it has been demonstrated for a PSA¹⁹ and IgG sandwich assay³³.

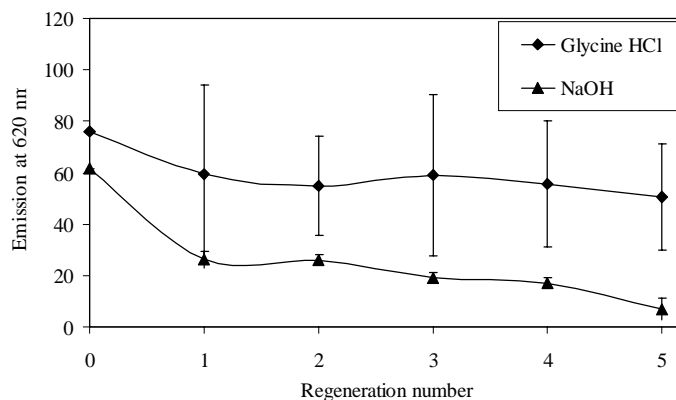


Figure 8. Fluorescence emission after sequential regeneration of ITO surface with different solvents

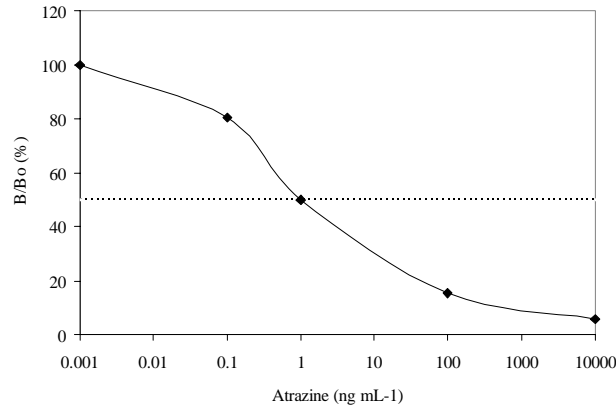


Figure 9. A standard curve for competitive inhibition assay of atrazine using a monoclonal Anti-Atrazine antibody (AM7B.2) coupled to 107 nm Seradyn particles. The assays were performed on an ITO waveguide. Dotted line indicates the IC₅₀.

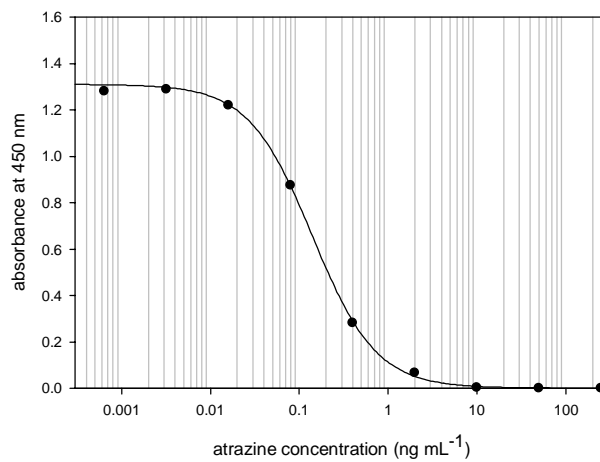


Figure 10. A 4-parameter curve fitting for the competitive 96-well plate immunoassay for atrazine using a monoclonal antibody (AM7B.2) (A: The highest emission; B: Slope of the linear region; C: IC₅₀ value (ng mL⁻¹); D: The lowest emission)

5 CONCLUSIONS

We have demonstrated the use of polystyrene nanoparticles with europium chelate as fluorescent reporters in an immunoassay for atrazine. Specifically, we were able to demonstrate that as the particle size decreases the time required for binding decreased and the sensitivity of the assay is increased. This suggests that the use of smaller particles would greatly speed up the reaction and simultaneously increase sensitivity. However, the detection system used sets limits to the particle size as well. There is clearly a point where standard detection system as a plate reader would not be sensitive enough to detect the emission from small particles. Therefore, a highly sensitive excitation/detection system as in ³⁷ needs to be developed to fully utilize the kinetic advantage from small particle size. This study shows the application of polystyrene nanoparticles with europium chelate for the detection of atrazine on an ITO waveguide. The results show that the sensitivity of the atrazine assay is similar to that of a conventional atrazine ELISA in a 96-well plate. ITO deposited on waveguide was shown to be an effective substrate for the assay with fluorescent polystyrene nanoparticles. To decrease the detection limit and create a highly sensitive biosensor, more tests need to be conducted to optimize the

antibody surface density on the particle surface. Based on other research, with a sandwich immunoassay for PSA the highest surface density provides the fastest assay¹⁹. In addition, the sensitivity of an immunoassay depends on the number of binding site on the particle surface³³. Therefore, it is essential to optimize the conjugation of an antibody to a particle for a competitive inhibition assay format. Future work will be focused on optimization of the assay within a microchannel.

Acknowledgments

The authors wish to acknowledge the support of the National Science Foundation, grant DBI-0102662 and the Superfund Basic Research Program with Grant 5P42ES04699 from the National Institute of Environmental Health Sciences, NIH with funding provided by EPA. The contents are solely the responsibility of the authors and do not necessarily represent the official views of the NIEHS, NIH or U.S. E.P.A.

REFERENCES

1. K. Pappaert, J. Vanderhoeven, P. Van Hummelen, B. Dutta, D. Clicq, G. V. Baron and G. Desmet, "Enhancement of DNA micro-array analysis using a shear-driven micro-channel flow system", *Journal of Chromatography A* **1014**, pp. 1-9, 2003.
2. O. Hofmann, G. Voirin, P. Niedermann and A. Manz, "Three-dimensional microfluidic confinement for efficient sample delivery to biosensor surfaces. Application to immunoassays on planar optical waveguides", *Analytical Chemistry* **74**, pp. 5243-5250, 2002.
3. J. S. Rossier, G. Gokulrangan, H. H. Girault, S. Svojanovsky and G. S. Wilson, "Characterization of protein adsorption and immunosorption kinetics in photoablated polymer microchannels", *Langmuir* **16**, pp. 8489-8494, 2000.
4. J. Schuderer, A. Akkoyun, A. Brandenburg, U. Bilitewski and E. Wagner, "Development of a multichannel fluorescence affinity sensor system", *Analytical Chemistry* **72**, pp. 3942-3948, 2000.
5. E. Eteshola and D. Leckband, "Development and characterization of an ELISA assay in PDMS microfluidic channels", *Sensors and Actuators B-Chemical* **72**, pp. 129-133, 2001.
6. M. L. Chabinyk, D. T. Chiu, J. C. McDonald, A. D. Stroock, J. F. Christian, A. M. Karger and G. M. Whitesides, "An integrated fluorescence detection system in poly(dimethylsiloxane) for microfluidic applications", *Analytical Chemistry* **73**, pp. 4491-4498, 2001.
7. P. A. Greenwood, C. Merrin, T. McCreedy and G. M. Greenway, "Chemiluminescence mu TAS for the determination of atropine and pethidine", *Talanta* **56**, pp. 539-545, 2002.
8. S. Koch, H. Wolf, C. Danapel and K. A. Feller, "Optical flow-cell multichannel immunosensor for the detection of biological warfare agents", *Biosensors & Bioelectronics* **14**, pp. 779-784, 2000.
9. V. Seidemann, J. Rabe, M. Feldmann and S. Buttgenbach, "SU8-micromechanical structures with in situ fabricated movable parts", *Microsystem Technologies* **8**, pp. 348-350, 2002.
10. K. Uchiyama, M. Yang, T. Sawazaki, H. Shimizu and S. Ito, "Development of a Bio-MEMS for Evaluation of dioxin toxicity by immunoassay method", *Sensors and Actuators B-Chemical* **103**, pp. 200-205, 2004.
11. Z. Liron, L. M. Tender, J. P. Golden and F. S. Ligler, "Voltage-induced inhibition of antigen-antibody binding at conducting optical waveguides", *Biosensors & Bioelectronics* **17**, pp. 489-494, 2002.
12. J. Feng, G. M. Shan, A. Maquieira, M. E. Koivunen, B. Guo, B. D. Hammock and I. M. Kennedy, "Functionalized europium oxide nanoparticles used as a fluorescent label in an immunoassay for atrazine", *Analytical Chemistry* **75**, pp. 5282-5286, 2003.
13. H. Harma, T. Soukka and T. Lovgren, "Europium nanoparticles and time-resolved fluorescence for ultrasensitive detection of prostate-specific antigen", *Clin Chem* **47**, pp. 561-8, 2001.
14. A. M. Pelkkikangas, S. Jaakohuhta, T. Lovgren and H. Harma, "Simple, rapid, and sensitive thyroid-stimulating hormone immunoassay using europium(III) nanoparticle label", *Analytica Chimica Acta* **517**, pp. 169-176, 2004.
15. P. von Lode, J. Rosenberg, K. Pettersson and H. Takalo, "A europium chelate for quantitative point-of-care immunoassays using direct surface measurement", *Analytical Chemistry* **75**, pp. 3193-3201, 2003.
16. T. Soukka, K. Anttonen, H. Harma, A. M. Pelkkikangas, P. Huhtinen and T. Lovgren, "Highly sensitive immunoassay of free prostate-specific antigen in serum using europium(III) nanoparticle label technology", *Clinica Chimica Acta* **328**, pp. 45-58, 2003.

17. T. Soukka, J. Paukkunen, H. Harma, S. Lonnberg, H. Lindroos and T. Lovgren, "Supersensitive time-resolved immunofluorometric assay of free prostate-specific antigen with nanoparticle label technology", *Clin Chem* **47**, pp. 1269-78, 2001.
18. G. J. Reimer, S. J. Gee and B. D. Hammock, "Comparison of a time-resolved fluorescence immunoassay and an enzyme-linked immunosorbent assay for the analysis of atrazine in water", *Journal of Agricultural and Food Chemistry* **46**, pp. 3353-3358, 1998.
19. T. Soukka, H. Harma, J. Paukkunen and T. Lovgren, "Utilization of kinetically enhanced monovalent binding affinity by immunoassays based on multivalent nanoparticle-antibody bioconjugates", *Analytical Chemistry* **73**, pp. 2254-2260, 2001.
20. H. Harma, T. Soukka, S. Lonnberg, J. Paukkunen, P. Tarkkinen and T. Lovgren, "Zeptomole detection sensitivity of prostate-specific antigen in a rapid microtitre plate assay using time-resolved fluorescence", *Luminescence* **15**, pp. 351-355, 2000.
21. K. Watanabe, H. Arakawa and M. Maeda, "Rapid simultaneous detection of verotoxin 1 and 2 using time-resolved fluoroimmunoassay", *Bunseki Kagaku* **51**, pp. 381-387, 2002.
22. M. Wortberg, S. B. Kreissig, G. Jones, D. M. Rocke and B. D. Hammock, "An Immunoarray for the Simultaneous Determination of Multiple Triazine Herbicides", *Analytica Chimica Acta* **304**, pp. 339-352, 1995.
23. A. E. Karu, R. O. Harrison, D. J. Schmidt, C. E. Clarkson, J. Grassman, M. H. Goodrow, A. Lucas, B. D. Hammock, J. M. Vanemon and R. J. White, "Monoclonal Immunoassay of Triazine Herbicides- Development and Implementation", *Acs Symposium Series* **451**, pp. 59-77, 1991.
24. L. L. Jaeger, A. D. Jones and B. D. Hammock, "Development of an enzyme-linked immunosorbent assay for atrazine mercapturic acid in human urine", *Chemical Research in Toxicology* **11**, pp. 342-352, 1998.
25. S. Z. Cohen, C. Eiden and M. N. Lorber, "Monitoring Groundwater for Pesticides", *Acs Symposium Series* **315**, pp. 170-196, 1986.
26. R. Loosli, *Rev. Environ. Contam. Toxicol.* **143**, pp. 47-57, 1995.
27. R. Renner, "Atrazine linked to endocrine disruption in frogs", *Environmental Science & Technology* **36**, pp. 55A-56A, 2002.
28. C. Yan, M. Zharnikov, A. Golzhauser and M. Grunze, "Preparation and characterization of self-assembled monolayers on indium tin oxide", *Langmuir* **16**, pp. 6208-6215, 2000.
29. C. K. Luscombe, H. W. Li, W. T. S. Huck and A. B. Holmes, "Fluorinated silane self-assembled monolayers as resists for patterning indium tin oxide", *Langmuir* **19**, pp. 5273-5278, 2003.
30. A. P. Fang, H. Ng, X. D. Su and S. F. Y. Li, "Soft-lithography-mediated submicrometer patterning of self-assembled monolayer of hemoglobin on ITO surfaces", *Langmuir* **16**, pp. 5221-5226, 2000.
31. D. Rodbard, *Ligand Assay*, Massin Publishing, New York, 1981.
32. J. O. Koskinen, J. Vaarno, N. J. Meltola, J. T. Soini, P. E. Hanninen, J. Luotola, M. E. Waris and A. E. Soini, "Fluorescent nanoparticles as labels for immunometric assay of creatine protein using two-photon excitation assay technology", *Analytical Biochemistry* **328**, pp. 210-218, 2004.
33. M. Hall, I. Kazakova and Y. M. Yao, "High sensitivity immunoassays using particulate fluorescent labels", *Anal Biochem* **272**, pp. 165-70, 1999.
34. C. J. Huang, Y. K. Su and S. L. Wu, "The effect of solvent on the etching of ITO electrode", *Materials Chemistry and Physics* **84**, pp. 146-150, 2004.
35. C. A. Huang, K. C. Li, G. C. Tu and W. S. Wang, "The electrochemical behavior of tin -doped indium oxide during reduction in 0.3 M hydrochloric acid", *Electrochimica Acta* **48**, pp. 3599-3605, 2003.
36. G. Folcher, H. Cachet, M. Froment and J. Bruneaux, "Anodic corrosion of indium tin oxide films induced by the electrochemical oxidation of chlorides", *Thin Solid Films* **301**, pp. 242-248, 1997.
37. C. Shi-Che, R. Peron, D. Dosev and I. M. Kennedy, "Time gated detection of europium nanoparticles in a micro channel based environmental immunoassay", *SPIE Proceedings, BioMEMS and Nanotechnology* **5275**, pp. 186-196, 2004.